THE JOURNAL OF PHYSICAL CHEMISTRY Letters

Letter

Cite This: J. Phys. Chem. Lett. 2018, 9, 1721−1727

pubs.acs.org/JPCL

Reproducing Quantum Probability Distributions at the Speed of Classical Dynamics: A New Approach for Developing Force-Field Functors

Vikram Sundar,*,† David Gelbwaser-Klimovsky,*,† and Alán Aspuru-Guzik*,†,‡

†Department of Chemistry and Chemical Biology, Harvard University, Cambridge, Massachusetts 02138, United States

‡Senior Fellow, Canadian Institute for Advanced Research, Toronto, Ontario M5G 1Z8, Canada

Supporting Information

ABSTRACT: Modeling nuclear quantum effects is required for accurate molecular dynamics (MD) simulations of molecules. The community has paid special attention to water and other biomolecules that show hydrogen bonding. Standard methods of modeling nuclear quantum effects like Ring Polymer Molecular Dynamics (RPMD) are computationally costlier than running classical trajectories. A force-field functor (FFF) is an alternative method that computes an effective force field that replicates quantum properties of the original force field. In this work, we propose an efficient method of computing FFF using the Wigner−Kirkwood expansion. As a test case, we calculate a range of thermodynamic properties of Neon, obtaining the same level of accuracy as RPMD, but with the shorter runtime of classical simulations. By modifying existing MD programs, the proposed method could be used in the future to increase the efficiency and accuracy of MD simulations involving water and proteins.

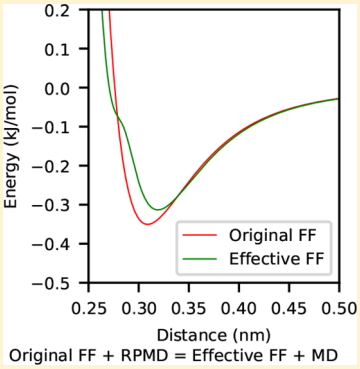

Biomolecular simulation methods have proven increasingly useful for understanding properties of biomolecules, such as protein binding and protein folding.[1,2] The most popular simulation methods today are molecular dynamics (MD) and Monte Carlo (MC) simulations, both of which rely on empirical force fields to model interactions between molecules.[1−3] Some modern force fields currently under development fit functional forms to the Born−Oppenheimer energy surface of the molecule, and other force fields use both data about the Born−Oppenheimer surface and experimental data.[3−6] Afterward, Monte Carlo and molecular dynamics are used to simulate atoms as classical particles moving on this Born−Oppenheimer surface,[6] ignoring quantum effects from the nuclear dynamics.

Accounting for nuclear quantum properties is essential for accurate biomolecular simulations using either molecular dynamics or Monte Carlo methods since they play a role in the thermodynamic properties of water and other fluids,[7,8] hydrogen-bonding[8] and the binding of enzymes to ligands.[9,10] Since Born−Oppenheimer force fields and classical MD do not account for these effects, a number of alternative methods have been developed to account for them. These include Path Integral Molecular Dynamics (PIMD),[6,11−13] Ring-Polymer Molecular Dynamics (RPMD),[14] Centroid Molecular Dynamics (CMD),[15] the generalized Langevin equation,[16] higher-order factorization schemes,[17,18] semiclassical initial value representation (SCIVR),[19] and other methods.[20,21] These methods have been used in simulations[20,22,23] but are slower than classical MD since they require an increase in the number of particles by a factor of 32 for hydrogen-containing systems at room temperature in order to achieve sufficient accuracy.[24]

In this Letter, we put forward an alternative method for performing quantum simulations at the speed of classical simulations with no loss in accuracy. In Babbush et al.,[25] we proved the existence and uniqueness of a force-field functor (FFF) that computes an effective potential that accounts for nuclear quantum corrections to the distribution function and can be used in classical simulations to calculate thermodynamic properties. Specifically, we defined the map $\mathcal{F}$ from a classical potential $V(q)$ with equilibrium quantum density $n_Q(q)$ to the effective potential $W(q)$ with equilibrium classical density $n_0(q) = n_Q(q)$. The path integral formulation of quantum mechanics allows us to explicitly write

$$W(q) = -\frac{1}{\beta}\log\left[\oint_{r(0)=q}^{r(\beta\hbar)=q} \mathcal{D}r(\tau)\, e^{-A[r(\tau)]}\right] \quad (1)$$

with Boltzmann factor β and Helmholtz free energy A. In Babbush et al.,[25] we demonstrated the existence of this map and showed its uniqueness.

$W(q)$ can be used to compute the equilibrium particle density and partition function, and thus all thermodynamic properties including imaginary-time nuclear quantum effects, at a cost equivalent to classical dynamics. Further, uniqueness of the FFF implies that any method of computing an effective

Received: December 8, 2017
Accepted: March 12, 2018
Published: March 12, 2018

DOI: 10.1021/acs.jpclett.7b03254
J. Phys. Chem. Lett. 2018, 9, 1721−1727

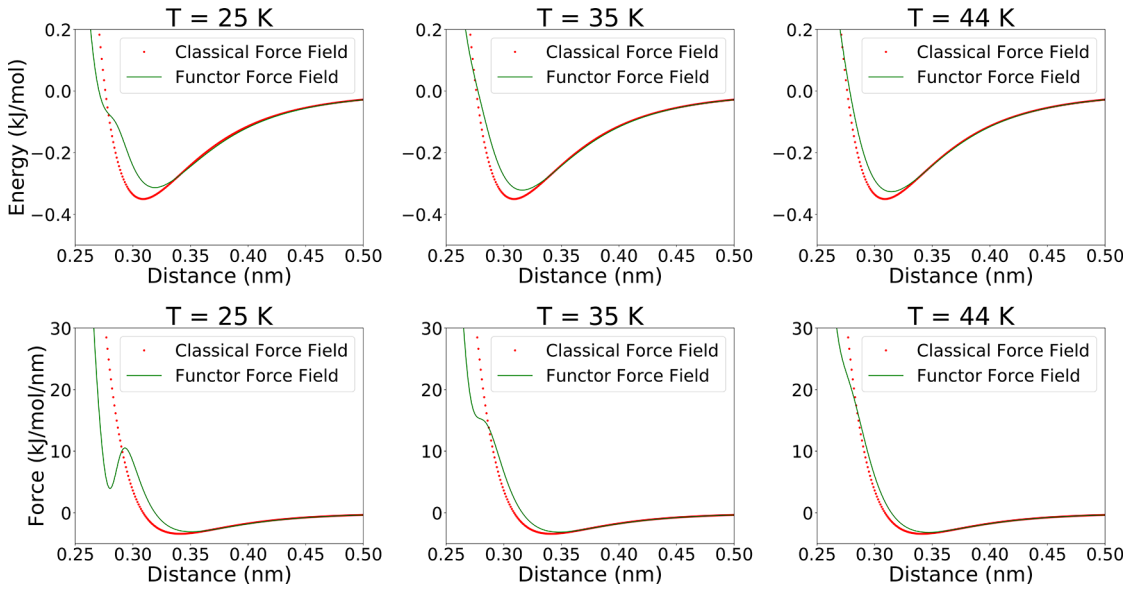

Figure 1. Classical and effective force field for Neon at T = 25 K, 35 K, and T = 44 K. The top plot shows the potential and the bottom plot shows the corresponding force. The red dotted curve is the classical potential from Hellmann et al.[41] and the green curve is the effective potential numerically computed using the Wigner expansion to second order. The change in shape and shallower well can be explained by the wavepacket entering the classically forbidden region and the zero-point energy, respectively.

potential that has the correct partition function and equilibrium density will satisfy these properties. However, the functor does not guarantee accurate computation of quantum dynamics[25] nor does it account for real-time quantum mechanical effects like tunneling and quantum resonances.[19] Should quantum dynamics be necessary, methods like RPMD or CMD should be used,[14,15] and should real-time quantum mechanical effects be necessary, methods like SCIVR should be used.[19]

We propose a method of computing the effective potential using the Wigner-Kirkwood expansion,[26,27] which was originally introduced to compute quantum corrections of thermal states. This expansion, when taken to infinite order, correctly reproduces the quantum partition function, so it must be the correct effective potential.[26,27]

Wigner[26] introduced the Wigner function to compute quantum corrections to a thermal state. The Wigner function of a thermal state of a particle in a potential $V(\vec{r})$ can be expanded as a function of $\hbar$

$$W(\vec{r}, \vec{p}) = e^{-\beta\mathcal{H}(\vec{r},\vec{p})}(1 + \beta^2\hbar^2 W_2(\vec{r}, \vec{p}) + \beta^4\hbar^4 W_4(\vec{r}, \vec{p}) + ...) \tag{2}$$

where $\mathcal{H}(\vec{r}, \vec{p})$ is the Hamiltonian and $\beta = \frac{1}{k_b T}$. The $W_i(\vec{r}, \vec{p})$ are functions of derivatives of the potential function $V(\vec{r})$; methods to compute them can be found in the studies of Wigner[26] and Coffey et al.[28] While other expansions of the quantum partition function do exist, the truncated Wigner expansion is known to be the best at reproducing quantum probability distributions along classical trajectories, so we chose it for our study.[29,30] The Wigner function can be used to compute the position-space probability distribution by integrating out the momentum coordinate. The effective potential, $\tilde{V}(\vec{r})$, that reproduces this distribution in a classical thermal state is then

$$\tilde{V}(\vec{r}) = -\frac{1}{\beta}\log\left[\int d\vec{p}\, W(\vec{r}, \vec{p})\right] \tag{3}$$

At high enough temperatures, any system behaves classically, and the Wigner function is equal to the classical phase space distribution, the first term in the Wigner expansion. At intermediate temperatures, quantum effects are relevant and are fully described by the first correction to the classical phase-space distribution, W_2.[26] For a spherically symmetric system, the non-normalized correction term is

$$W_2(r, p, \theta) = \frac{1}{24m^2 r}\left(-6m\frac{\partial V}{\partial r} + \beta p^2 \sin^2\theta\frac{\partial V}{\partial r} + mr\beta\left(\frac{\partial V}{\partial r}\right)^2 - 3mr\frac{\partial^2 V}{\partial r^2} + \beta p^2 r\cos^2\theta\frac{\partial^2 V}{\partial r^2}\right) \tag{4}$$

Here, r is radial distance, p is the magnitude of the momentum, and θ is the angle between position and momentum.

In a simulation, the true potential is a function of all N atoms, not just two. Nevertheless, under the appropriate conditions, the effective potential may still be approximated as the pairwise additive sum of the corrected potential computed in eq 4. The approximations required for this to hold and verification of those approximations for our test case of a Neon force field may be found in the Supporting Information. These approximations become increasingly accurate at higher temperatures.

For our analysis to hold, the force field must have previously been fit to high-quality electronic structure data. This will ensure that the initial classical force field accurately models dynamics according to the electronic structure. We can then use the Born−Oppenheimer approximation to isolate nuclear and electronic effects and use the FFF to add nuclear quantum effects. Many popular force fields, like CHARMM or AMBER, are fitted to experimental data like the radial distribution function, heat of vaporization, or density, which already account for nuclear quantum effects;[31,32] using the FFF or other quantum simulation methods on these force fields would double-count those effects.[33] However, these force fields have

DOI: 10.1021/acs.jpclett.7b03254
J. Phys. Chem. Lett. 2018, 9, 1721−1727

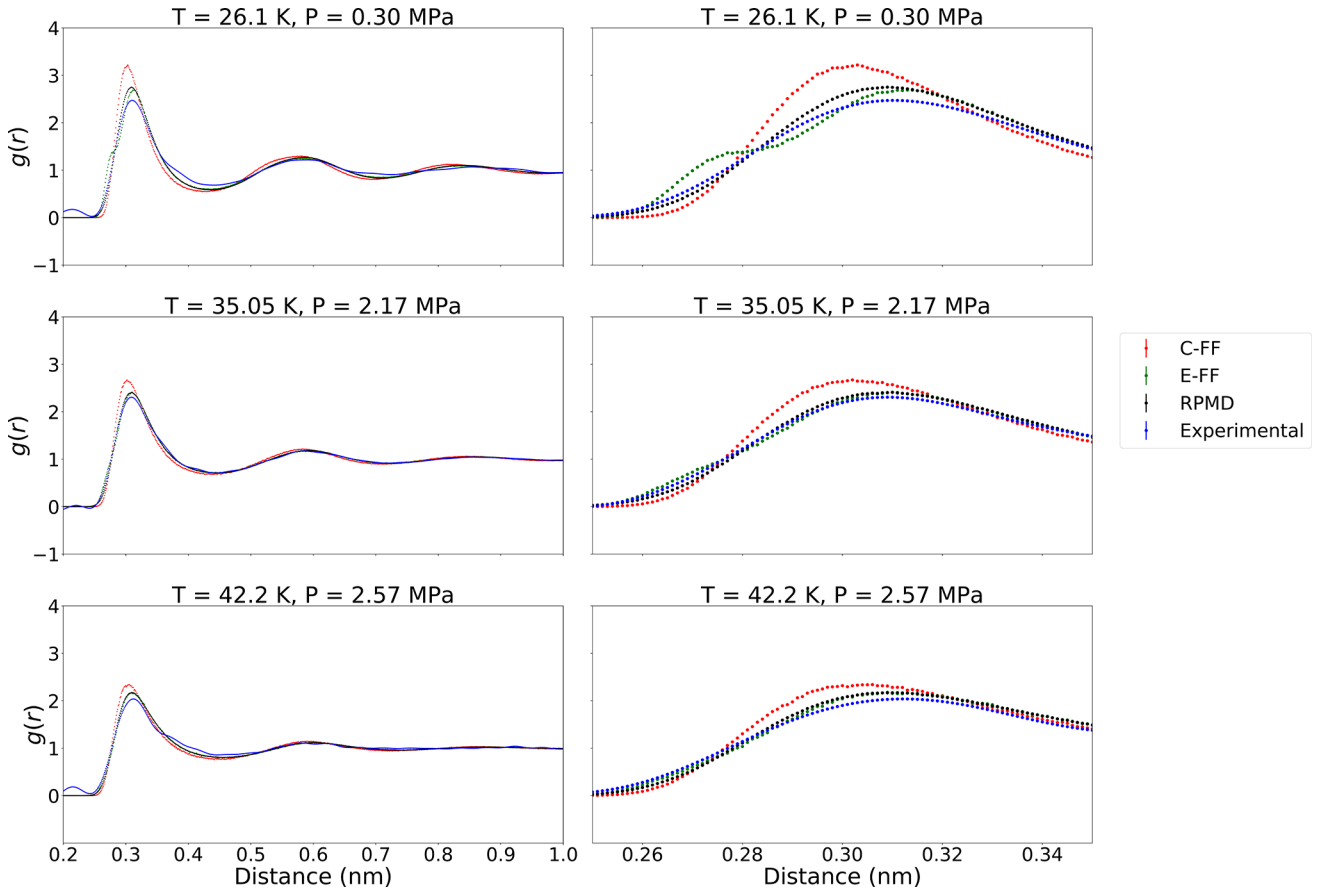

Figure 2. Radial distribution function as computed by C-FF, E-FF, and RPMD. In each plot, the red curve is computed by C-FF, the green curve is computed by E-FF, the black curve is computed by RPMD, and the blue curve is experimentally determined from Bellissent-Funel et al.[42] and de Graaf and Mozer.[43] The right side focuses on just the first peak. In all cases, the height and location of the first peak are more accurately determined by E-FF and RPMD than by C-FF. E-FF demonstrates similar accuracy as the significantly slower RPMD.

generally had limited transferability in measuring experimental parameters that they are not fitted to.

Previous efforts to use Wigner−Kirkwood expansions to add quantum corrections to MD calculations have had mixed results. Instead of using an effective potential, many of these efforts[6,34−39] added quantum corrections to thermodynamic quantities after the simulation. This approach is more time-consuming, since corrections need to be computed for every thermodynamic quantity of interest.[6] Ermakova et al.[40] used an effective potential on a Neon force field fitted to low-quality electronic structure data, so their results, particularly the position of the radial distribution function of nearest-neighbor peaks, did not show an unambiguous improvement over the classical potential. We demonstrate that an effective potential derived from high-quality *ab initio* data can be used to calculate condensed-phase properties with high accuracy and significant improvements over classical calculations.

We test our method on a Neon force field. Neon's interatomic potential is spherically symmetric, and a highly accurate force field for Neon was derived by Hellmann et al.[41] by fitting functional forms to high-quality CCSD(T) electronic structure data.

We began by numerically computing the effective potential at various temperatures as shown in Figure 1. We note two characteristics of the effective potential, which can be explained by quantum phenomena: First, the repulsive wall as $r \to 0$ is less steep in the effective potential than in the classical potential. This is due to the fact that the quantum wavepacket can enter the classically forbidden region $E < V(r)$. Second, the well is shallower, due to the zero-point energy.

Moreover, the equilibrium distance is slightly longer in the effective potential than in the classical potential. As we show below, this has important thermodynamic consequences.

We note a bump in the effective force field at $T = 25$ K. This is likely an artifact due to use of only the second-order expansion and neglecting the N-body terms, and not a reflection of the full quantum effective force field. This bump is also significantly larger in the effective force than in the potential. Addition of subsequent terms in the Wigner expansion help eliminate this bump, as shown in the Supporting Information.[38]

Figure 2 shows radial distribution functions (RDF) for liquid Neon at $T = 26.1$ K, $T = 35.05$ K, and $T = 42.2$ K. Experimental data[42,43] is compared to three simulation methods: a classical MD simulation with the classical force field (henceforth called C-FF); a standard RPMD simulation with the classical force field, which accounts for nuclear quantum effects (henceforth called RPMD); and a classical MD simulation with the effective force field (henceforth called E-FF).

At $T = 35.05$ K and $T = 42.2$ K, E-FF is roughly as accurate as RPMD, with both being a significant improvement relative to C-FF. In particular, the location and height of the first peak obtained by E-FF are more precise than those derived by C-FF. The shift and lower height of the peak are caused by quantum

DOI: 10.1021/acs.jpclett.7b03254
J. Phys. Chem. Lett. 2018, 9, 1721−1727

corrections, which shift the equilibrium position and reduce the depth of the well in the effective potential described above.

At T = 26.1 K, E-FF, while still a significant improvement over C-FF, is somewhat worse than RPMD. Specifically, the location and height of the peak are relatively accurate, but the bump in the potential noted above results in a similar bump in the RDF. Inaccuracies in both RPMD and E-FF at this temperature indicate more beads, higher-order terms, and a more accurate electronic structure potential are necessary for an accurate computation of the RDF.

We also measured the location of the first peak of the radial distribution function and compare our results with those of Ermakova et al.[40] in Table 1. As noted earlier, we demonstrate clear, consistent improvement in our computed radial distribution function from C-FF to E-FF and moderate improvement over the results computed by Ermakova et al.[40] This emphasizes the need of high-quality electronic data in order to obtain accurate radial distribution functions.

Table 1. Position of the First Peak of the RDF[a]

temperature	26 K	35 K	42 K
our C-FF	303 pm	302 pm	306 pm
our E-FF	313 pm	310 pm	309 pm
Ermakova et al.[40] C-FF	306 pm	307 pm	308 pm
Ermakova et al.[40] E-FF	314 pm	312 pm	312 pm
experimental	310 pm	310 pm	310 pm

[a]Our results (E-FF) are closer to the experimental data than C-FF and previous results.[40]

RPMD is around 32 times slower on similar-capability machines than E-FF. This is expected since RPMD has P = 32 beads per atom and RPMD simulations scale as $O(VP)$ where V is the cost of the potential and P is the number of beads per atom. Thus, E-FF reproduces the results of quantum simulations at the significantly faster speed of classical simulations. Computing speed is especially relevant for more complex calculations such as the equation of state and vapor−liquid coexistence curve.

Figure 3 shows the equation of state for Neon at T = 36 K and T = 40 K. Experimental data[44] is compared to densities from NPT MD simulations for both the classical and effective potential.[45] These values span liquid and gas phase.

Both E-FF and C-FF were accurate on gas-phase densities. The maximum error relative to the experimental data for C-FF is around 1% and for E-FF around 2%. This is somewhat expected since gas-phase densities do not depend much on the force field; we see that the ideal gas term (independent of potential) dominates in the equation of state relative to the virial coefficients (which depend on potential). In liquid phase, C-FF significantly overestimates the experimental density by as much as 10% while E-FF only overestimates the experimental density by around 2%. This is due to the shift in equilibrium position described above. Adding additional terms to the Wigner expansion should further reduce the error in calculated density.

We computed the vapor−liquid coexistence curve with Gibbs Monte Carlo simulations for both the classical and effective potential.[47−50] Experimental data for both densities and pressures was obtained from Rabinovich et al.[46] We ran simulations ranging from close to the triple point to close to the critical point, thus covering the entire range of the vapor−liquid coexistence curve.

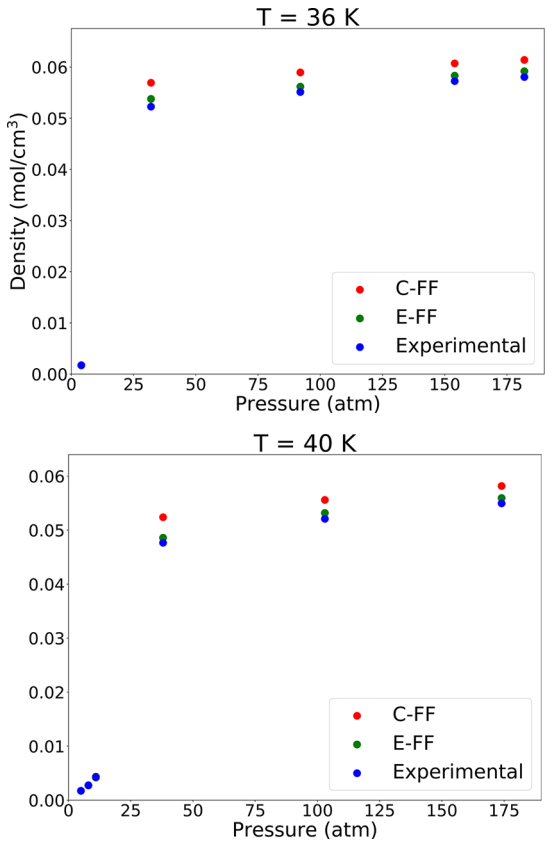

Figure 3. Equation of state as computed by C-FF and E-FF at T = 36 K, 40 K. The red points were computed by C-FF, the green points by E-FF, and the blue points were experimentally determined by Gibbons.[44] The gas-phase density points from all three methods are too close to be distinguished. E-FF is significantly more accurate in liquid-phase, reducing the error relative to experimental data from 10% for C-FF to 2% for E-FF.

E-FF is significantly more accurate in determining both the density and the pressure of the vapor−liquid coexistence point, as shown in Figure 4. Figure 4a,b plots the computed vapor−liquid coexistence curve as density versus temperature and as temperature versus pressure; Figure 4c,d plots the errors in density and pressure, respectively, as a function of density and temperature. C-FF consistently overestimates the liquid density by an average percent error of 12% relative to experimental data, while E-FF consistently overestimates it by only 5%. This effect can be partly explained by the density deviations observed when computing the equation of state. C-FF underestimates gas density by an average percent error of 40% relative to the experimental data, while E-FF underestimates it by 11%. Finally, C-FF underestimates the pressure by an average percent error of 33% relative to the experimental data, while E-FF underestimates it by 7%. Larger errors at lower temperature suggest that the effective force field would be improved by using higher-order corrections (see eq 2).

We also note that E-FF began exhibiting critical behavior, i.e., transitions between vapor and liquid phase, at around T = 43 K, very close to the experimental critical point of T_c = 44.40 K. C-FF did not exhibit similar behavior even at T = 44 K. We chose not to measure the critical point directly due to inaccuracies with Gibbs MC simulations close to the critical point,[51] but this result suggests that C-FF also overestimates the critical point.

DOI: 10.1021/acs.jpclett.7b03254
J. Phys. Chem. Lett. 2018, 9, 1721−1727

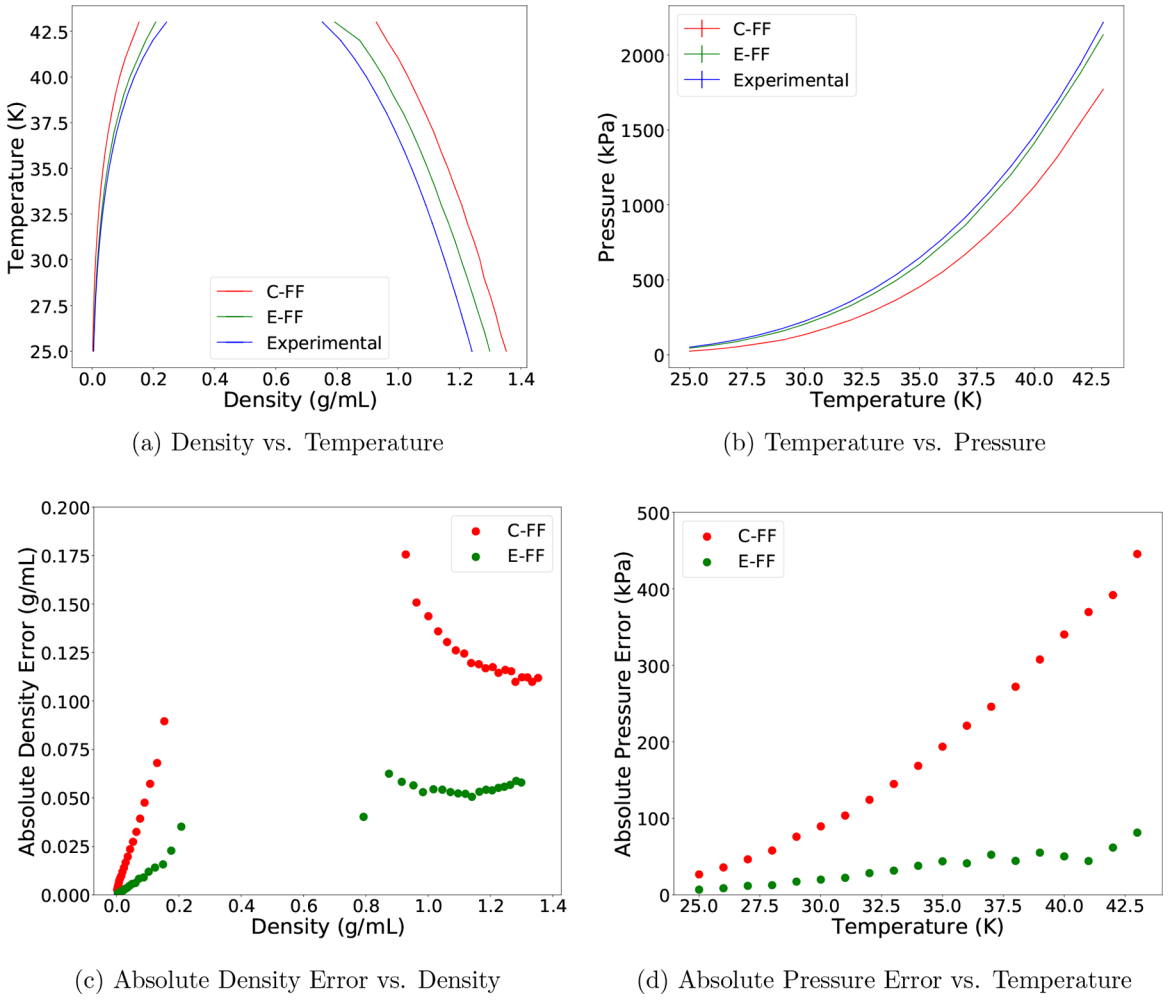

(a) Density vs. Temperature

(b) Temperature vs. Pressure

(c) Absolute Density Error vs. Density

(d) Absolute Pressure Error vs. Temperature

Figure 4. Vapor−liquid coexistence curve for Neon, as computed by Gibbs MC simulation with both C-FF and E-FF. The red curves are computed by C-FF, the green curves by E-FF, and the blue curves were experimentally determined by Rabinovich et al.[46] E-FF is significantly more accurate in all cases. It reduces the average error relative to the experimental data: from 40% to 11% for the gas phase density; from 12% to 5% for the liquid phase density; from 33% to 7% for the pressure. The aberrant point in panel c is due to simulation errors close to the critical point.

Our results conclusively show that the effective force field is significantly more accurate than the classical force field for Neon on a wide range of condensed-phase parameters. We have also demonstrated that the effective force field was capable of computing radial distribution functions to the same degree of accuracy as quantum simulations with the speed of a classical simulation, i.e., the FFF can be used to account for nuclear quantum effects about a hundred times faster than standard methods. The FFF can be applied to any force field that is fitted to sufficiently high-quality quantum energy data and for which subsequent terms in the Wigner expansion can reasonably be suppressed to accurately account for nuclear quantum effects at the speed of a classical simulation.

Next steps include extending this method to nonspherical force fields and force fields for biomolecules, which are relevant to biochemists. The Supporting Information includes a section about the additional approximations that must be made to extend our method to pairwise additive potentials for general *N*-particle systems; these were valid for the Neon force field used here but must be verified for other force fields.

The FFF could significantly correct simulations for any biomolecule involving hydrogen bonding or hydrogen atoms in a central way, including water, proteins, and nucleic acids.[7−10] Applying the FFF to protein or water force fields fit to high-quality electronic structure data should result in accurate quantum simulations of biomolecules with no additional computational cost.

■ ASSOCIATED CONTENT

Supporting Information

The Supporting Information is available free of charge on the ACS Publications website at DOI: 10.1021/acs.jpclett.7b03254.

Details of simulation methods; justification of approximations made in the Wigner expansion, such as the use of a pairwise-additive 2-body potential to model an *N*-body system and the omission of higher-order terms in the expansion; description of how to extend our work to more complicated potentials (PDF)

A *Mathematica* notebook demonstrating how to compute the effective potential (ZIP)

■ AUTHOR INFORMATION

Corresponding Authors

*E-mail: vikramsundar@college.harvard.edu.
*E-mail: dgelbwaser@fas.harvard.edu.
*E-mail: alan@aspuru.com.

DOI: 10.1021/acs.jpclett.7b03254
J. Phys. Chem. Lett. 2018, 9, 1721−1727

ORCID

Alán Aspuru-Guzik: 0000-0002-8277-4434

Notes

The authors declare no competing financial interest.

■ ACKNOWLEDGMENTS

This project was partially funded by a grant from the Harvard College Research Program, a grant from the Harvard University Center for the Environment Undergraduate Research Fund, and a grant from the Harvard Physics Department. D.G.-K. and A.A.-G. acknowledge the support from the Center for Excitonics, an Energy Frontier Research Center funded by U.S. Department of Energy under award DE-SC0001088. Numerical simulations for this project were run on the Harvard Odyssey cluster.

■ REFERENCES

(1) Dror, R. O.; Dirks, R. M.; Grossman, J. P.; Xu, H.; Shaw, D. E. Biomolecular Simulation: A Computational Microscope for Molecular Biology. *Annu. Rev. Biophys.* **2012**, *41*, 429−452.

(2) Mura, C.; McAnany, C. E. An Introduction to Biomolecular Simulations and Docking. *Mol. Simul.* **2014**, *40*, 732−764.

(3) González, M. A. Force Fields and Molecular Dynamics Simulations. *Collection SFN* **2011**, *12*, 169−200.

(4) Lopes, P. E. M.; Guvench, O.; MacKerell, A. D. Current Status of Protein Force Fields for Molecular Dynamics. *Methods Mol. Biol.* **2015**, *1215*, 47−71.

(5) Chu, H.; Cao, L.; Peng, X.; Li, G. Polarizable Force Field Development for Lipids and Their Efficient Applications in Membrane Proteins. *WIREs Comput. Mol. Sci.* **2017**, *7*, e1312.

(6) Allen, M.; Tildesley, D. J. *Computer Simulation of Liquids*; Clarendon Press: Oxford, U.K., 1987.

(7) Ceriotti, M.; Fang, W.; Kusalik, P. G.; McKenzie, R. H.; Michaelides, A.; Morales, M. A.; Markland, T. E. Nuclear Quantum Effects in Water and Aqueous Systems: Experiment, Theory, and Current Challenges. *Chem. Rev.* **2016**, *116*, 7529−7550.

(8) Raugei, S.; Klein, M. L. Nuclear Quantum Effects and Hydrogen Bonding in Liquids. *J. Am. Chem. Soc.* **2003**, *125*, 8992−8993.

(9) Agarwal, P. K.; Billeter, S. R.; Hammes-Schiffer, S. Nuclear Quantum Effects and Enzyme Dynamics in Dihydrofolate Reductase Catalysis. *J. Phys. Chem. B* **2002**, *106*, 3283−3293.

(10) Wang, M.; Lu, Z.; Yang, W. Nuclear Quantum Effects on an Enzyme-Catalyzed Reaction with Reaction Path Potential: Proton Transfer in Triosephosphate Isomerase. *J. Chem. Phys.* **2006**, *124*, 124516.

(11) Chandler, D.; Wolynes, P. G. Exploiting the Isomorphism between Quantum Theory and Classical Statistical Mechanics of Polyatomic Fluids. *J. Chem. Phys.* **1981**, *74*, 4078−4095.

(12) Fosdick, L. D.; Jordan, H. F. Path Integral Calculation of the Two Particle Slater Sum for Helium. *Phys. Rev.* **1966**, *143*, 58−66.

(13) Fanourgakis, G. S.; Markland, T. E.; Manolopoulos, D. E. A Fast Path Integral Method for Polarizable Force Fields. *J. Chem. Phys.* **2009**, *131*, 094102.

(14) Habershon, S.; Manolopoulos, D. E.; Markland, T. E.; Miller, T. F. Ring-Polymer Molecular Dynamics: Quantum Effects in Chemical Dynamics from Classical Trajectories in an Extended Phase Space. *Annu. Rev. Phys. Chem.* **2013**, *64*, 387−413.

(15) Pavese, M.; Jang, S.; Voth, G. A. Centroid Molecular Dynamics: A Quantum Dynamics Method Suitable for the Parallel Computer. *Parallel Computing* **2000**, *26*, 1025−1041.

(16) Ceriotti, M.; Manolopoulos, D. E.; Parrinello, M. Accelerating the Convergence of Path Integral Dynamics with a Generalized Langevin Equation. *J. Chem. Phys.* **2011**, *134*, 084104.

(17) Jang, S.; Jang, S.; Voth, G. A. Applications of Higher Order Composite Factorization Schemes in Imaginary Time Path Integral Simulations. *J. Chem. Phys.* **2001**, *115*, 7832−7842.

(18) Pérez, A.; Tuckerman, M. E. Improving the Convergence of Closed and Open Path Integral Molecular Dynamics via Higher Order Trotter Factorization Schemes. *J. Chem. Phys.* **2011**, *135*, 064104.

(19) Miller, W. H. The Semiclassical Initial Value Representation: A Potentially Practical Way for Adding Quantum Effects to Classical Molecular Dynamics Simulations. *J. Phys. Chem. A* **2001**, *105*, 2942−2955.

(20) Nakayama, A.; Makri, N. Forward-Backward Semiclassical Dynamics for Quantum Fluids using Pair Propagators: Application to Liquid *para*-Hydrogen. *J. Chem. Phys.* **2003**, *119*, 8592−8605.

(21) Poulsen, J. A.; Nyman, G.; Rossky, P. J. Practical Evaluation of Condensed-Phase Quantum Correlation Functions: A Feynman-Kleinert Variational Linearized Path Integral Method. *J. Chem. Phys.* **2003**, *119*, 12179.

(22) Paesani, F.; Zhang, W.; Case, D. A.; Cheatham, T. E.; Voth, G. A. An Accurate and Simple Quantum Model for Liquid Water. *J. Chem. Phys.* **2006**, *125*, 184507.

(23) Liu, J.; Miller, W. H.; Paesani, F.; Zhang, W.; Case, D. A. Quantum Dynamical Effects in Liquid Water: A Semiclassical Study on the Diffusion and the Infrared Absorption Spectrum. *J. Chem. Phys.* **2009**, *131*, 164509.

(24) Markland, T. E.; Manolopoulos, D. E. An Efficient Ring Polymer Contraction Scheme for Imaginary Time Path Integral Simulations. *J. Chem. Phys.* **2008**, *129*, 024105.

(25) Babbush, R.; Parkhill, J.; Aspuru-Guzik, A. Force-field Functor Theory: Classical Force Fields Which Reproduce Equilibrium Quantum Distributions. *Front. Chem.* **2013**, *1*, 26.

(26) Wigner, E. On the Quantum Correction for Thermodynamic Equilibrium. *Phys. Rev.* **1932**, *40*, 749−759.

(27) Kirkwood, J. G. Quantum Statistics of Almost Classical Assembles. *Phys. Rev.* **1933**, *44*, 31−37.

(28) Coffey, W. T.; Kalmykov, Y. P.; Titov, S. V.; Mulligan, B. P. Wigner Function Approach to the Quantum Brownian Motion of a Particle in a Potential. *Phys. Chem. Chem. Phys.* **2007**, *9*, 3361−3382.

(29) Lee, H.-W. Theory and Application of the Quantum Phase-Space Distribution Functions. *Phys. Rep.* **1995**, *259*, 147−211.

(30) O'Connell, R. F.; Wang, L.; Williams, H. A. Time Dependence of a General Class of Quantum Distribution Functions. *Phys. Rev. A: At., Mol., Opt. Phys.* **1984**, *30*, 2187−2192.

(31) Brooks, B. R.; Brooks, C. L.; MacKerell, A. D.; Nilsson, L.; Petrella, R. J.; Roux, B.; Won, Y.; Archontis, G.; Bartels, C.; Caflisch, A.; et al. CHARMM: The Biomolecular Simulation Program. *J. Comput. Chem.* **2009**, *30*, 1545−1614.

(32) Ponder, J. W.; Case, D. A. Force Fields for Protein Simulations. *Adv. Protein Chem.* **2003**, *66*, 27−85.

(33) Spura, T.; John, C.; Habershon, S.; Kuhne, T. D. Nuclear Quantum Effects in Liquid Water from Path-Integral Simulations using an Ab Initio Force Matching Approach. *Mol. Phys.* **2015**, *113*, 808−822.

(34) Barker, J. A.; Fisher, R. A.; Watts, R. O. Liquid Argon: Monte Carlo and Molecular Dynamics Simulations. *Mol. Phys.* **1971**, *21*, 657−673.

(35) Barocchi, F.; Neumann, M.; Zoppi, M. Molecular-Dynamics Calculation of the Quantum Correction to the Pair-Distribution Function for a Lennard-Jones Fluid. *Phys. Rev. A: At., Mol., Opt. Phys.* **1984**, *29*, 1331−1334.

(36) Matsui, M. Molecular Dynamics Study of the Structural and Thermodynamic Porperties of MgO Crystal with Quantum Correction. *J. Chem. Phys.* **1989**, *91*, 489−494.

(37) Barocchi, F.; Neumann, M.; Zoppi, M. Wigner-Kirkwood Expansion: Calculation of "Almost Classical" Static Properties of a Lennard-Jones Many-Body System. *Phys. Rev. A: At., Mol., Opt. Phys.* **1987**, *36*, 2440−2454.

(38) Neumann, M.; Zoppi, M. Asymptotic Expansions and Effective Potentials for Almost Classical N-body Systems. *Phys. Rev. A: At., Mol., Opt. Phys.* **1989**, *40*, 4572−4584.

(39) Barocchi, F.; Neumann, M.; Zoppi, M. Quantum-Corrected Pair Distribution Function of Liquid Neon. *Phys. Rev. A: At., Mol., Opt. Phys.* **1985**, *31*, 4015−4017.

DOI: 10.1021/acs.jpclett.7b03254
J. Phys. Chem. Lett. 2018, 9, 1721−1727

(40) Ermakova, E.; Solca, J.; Huber, H.; Marx, D. Many-body and Quantum Effects in the Radial Distribution Function of Liquid Neon and Argon. *Chem. Phys. Lett.* **1995**, *246*, 204−208.
(41) Hellmann, R.; Bich, E.; Vogel, E. *Ab initio* potential energy curve for the Neon atom pair and thermophysical properties of the dilute Neon gas. I. Neon-Neon interatomic potential and rovibrational spectra. *Mol. Phys.* **2008**, *106*, 133−140.
(42) Bellissent-Funel, M. C.; Buontempo, U.; Filabozzi, A.; Petrillo, C.; Ricci, F. P. Neutron diffraction of liquid Neon and xenon along the coexistence line. *Phys. Rev. B: Condens. Matter Mater. Phys.* **1992**, *45*, 4605−4613.
(43) de Graaf, L. A.; Mozer, B. Structure Study of Liquid Neon by Neutron Diffraction. *J. Chem. Phys.* **1971**, *55*, 4967−4973.
(44) Gibbons, R. M. The Equation of State of Neon between 27 and 70 K. *Cryogenics* **1969**, *9*, 251−260.
(45) Eastman, P.; Friedrichs, M. S.; Chodera, J. D.; Radmer, R. J.; Bruns, C. M.; Ku, J. P.; Beauchamp, K. A.; Lane, T. J.; Wang, L.-P.; Shukla, D.; et al. OpenMM 4: A Reusable, Extensible, Hardware Independent Library for High Performance Molecular Simulation. *J. Chem. Theory Comput.* **2013**, *9*, 461−469.
(46) Rabinovich, V. A.; Vasserman, A. A.; Nedostup, V. I.; Veksler, L. S. *Thermophysical Properties of Neon, Argon, Krypton, and Xenon*; National Standard Reference Data Service of the USSR: A Series of Property Tables; Hemisphere Publishing Corporation: Carlsbad, CA, 1988; Vol. *10*.
(47) Panagiotopoulos, A. Z. Direct Determination of Phase Coexistence Properties of Fluids by Monte Carlo Simulation in a New Ensemble. *Mol. Phys.* **1987**, *61*, 813−826.
(48) Panagiotopoulos, A. Z.; Quirke, N.; Stapleton, M.; Tildesley, D. J. Phase Equilibria by Simulation in the Gibbs Ensemble. *Mol. Phys.* **1988**, *63*, 527−545.
(49) Morales, A. D. C.; Economou, I. G.; Peters, C. J.; Siepmann, J. I. Influence of Simulation Protocols on the Efficiency of Gibbs Ensemble Monte Carlo Simulations. *Mol. Simul.* **2013**, *39*, 1135−1142.
(50) Martin, M. G. MCCCS Towhee: ATool for Monte Carlo Molecular Simulation. *Mol. Simul.* **2013**, *39*, 1212−1222.
(51) Dinpajooh, M.; Bai, P.; Allan, D. A.; Siepmann, J. I. Accurate and Precise Determination of Critical Properties from Gibbs Ensemble Monte Carlo Simulations. *J. Chem. Phys.* **2015**, *143*, 114113.

DOI: 10.1021/acs.jpclett.7b03254
J. Phys. Chem. Lett. 2018, 9, 1721−1727